

Localized Geomagnetic Field Changes Near Active Faults in California 1974-1980

PAUL M. DAVIS

Department of Earth and Space Sciences, University of California, Los Angeles

MALCOLM J. S. JOHNSTON

U.S. Geological Survey

Daily averages of magnetic difference fields for the years 1974-1980 between 23 magnetometers on the San Andreas fault (between San Francisco and the Mexican border) have been analyzed to isolate the geomagnetic variation of crustal origin and to test if it is related to stress. Field changes due to nonuniform secular variation from currents in the core have been identified and removed. External currents in the ionosphere and magnetosphere induce changes in the difference fields due to contrasting impedances at magnetometer sites. These changes are identified and removed by multichannel predictive filtering using Boulder magnetic observatory component fields as inputs to the prediction operator. The remaining fluctuations (up to several nT) are attributed to crustal magnetization changes. Evidence that these changes are stress related includes the variation prior to the Busch fault earthquake (1974) seen at the two stations closest to (within 10 km) the epicenter. Also, stations within 50 km of the 1979 Coyote earthquake undergo localized field change up to a year before that event. If truly precursive, these variations are on a broader spatial and temporal scale than those for the Busch fault event. During the period 1975-1978 the geomagnetic variation is approximately uniform across the array, without the development of any significant anomalies. This period roughly coincides with the 1975.7-1978.7 seismic lull in nearly all of California. It is followed by a marked increase in crustal secular variation. Long-range coherence between anomalous variation at different stations is not seen, other than the variation before the Busch fault earthquake, suggesting that localized variation occurs on a scale of less than 10 km. Coseismic tectonomagnetic events are not observed at the times of the Busch and Coyote earthquakes, but model calculations suggest that observable events are not expected. If the observed changes are due to stress, they indicate that changes of aseismic stress are significantly larger than coseismic stress release.

INTRODUCTION

During the first year of operation of the U.S. Geological Survey magnetometer array (1974) an anomalous excursion of 2 nT was seen in the records from a recording magnetometer (labelled SJ in Figure 1). The excursion persisted for nearly 1 month, ending 4 weeks before the Busch fault earthquake ($M_L = 5.1$) of November 28, 1974 [Smith and Johnston, 1976]. Subsequently, it was shown using predictive filtering [Davis et al., 1980] that an anomalous excursion occurred during the same interval at another magnetometer site (AN in Figure 1) on the San Andreas fault. Of the six sites operating at the time, these two lie closest to the epicenter, each at a distance of approximately 10 km. If the anomalous variation is ascribed to stress-induced piezomagnetic effects in the crust, the observations suggest that a regional stress concentration formed on the San Andreas fault over a 10-km-scale length. This concentration then relaxed, loading the Busch fault and giving rise to the ensuing earthquake [Johnston, 1978].

Following these observations, the array was extended to its current 28 stations, continuously recording the earth's total magnetic field in the region between San Francisco and the Mexican border (Figure 1). A second moderate earthquake, the Coyote Lake earthquake ($M_L = 5.7$), occurred within the array on August 6, 1979. However, variations similar to those before the Busch fault earthquake were not observed immediately prior to that event [Johnston et al., 1981]. In this study we analyze records from the extended array, using the predictive filtering technique [Davis et al., 1981] to see if the vari-

ation before the Busch fault earthquake can still be regarded as precursive and if long-term anomalies were associated with the Coyote earthquake.

THE DATA SET

The stations shown in Figure 1 consist of continuously recording proton precession magnetometers (Geometrics) of 0.25-nT resolution. Readings are made once every 10 minutes and are telemetered to Menlo Park, where differences are taken between simultaneous readings at adjacent and nearly adjacent stations. There are 36 differences formed routinely from the 23 magnetometers used in this study. These differences are largely free of fluctuations due to external fields arising from currents in the ionosphere and magnetosphere. Such fields originate from distant currents and are nearly uniform at closely spaced stations. Differencing virtually cancels these fluctuations. The part remaining can be further reduced by methods of multichannel Wiener predictive filtering, with the filters giving the relative impedances between sites. Our analysis deals with the daily averages of difference fields, with the restriction that unless over 50% of the daily differences are of good quality (i.e., lie between the mean value ± 50 nT), the data for that day are flagged and not used.

THE ELIMINATION OF NONLOCAL FLUCTUATIONS

Variations in the difference fields are thought to arise principally from three sources: external currents and their associated induced fields in the earth, variations in internal currents in the core, and changes in crustal magnetization due to stress. The key to recognizing stress-induced variation lies in eliminating changes from the other two sources. The effects of currents of external origin can be treated by defining filters which, convolved with component field records, can predict the total

Copyright 1983 by the American Geophysical Union.

Paper number 3B1066.
0148-0227/83/003B-1066\$05.00

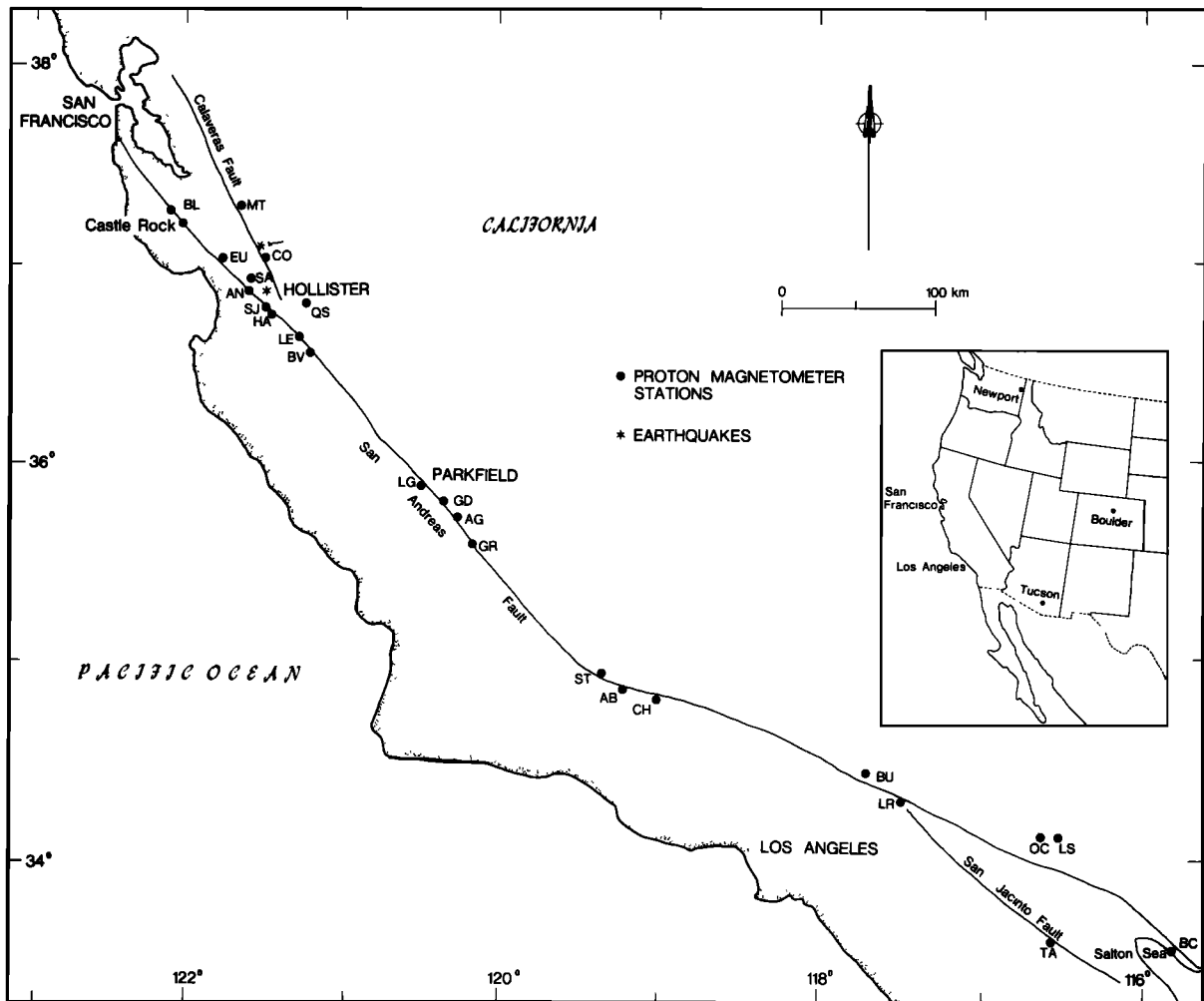


Fig. 1. Map of the U.S. Geological total field magnetometer array. Epicentral positions of the Busch fault 1974 (near AN) and Coyote 1979 (near CO) earthquakes are marked with asterisks. Inset shows the locations of the magnetic observatories Boulder, Newport, and Tucson.

field differences as a function of time. Currents of internal origin give rise to different secular variation rates at different sites. This variation can be removed because it is spatially smooth, allowing a good least squares estimate of its contribution. However, in crustal rocks of varying magnetic susceptibility, the core fields induce fields that give rise to an apparent secular variation. When differences are taken between closely spaced stations, the core components nearly cancel so that the crustal component can dominate the long-term trend. The filters determined from the external activity can be used to correct for this crustal component by using the core field components as inputs.

Component field data were obtained from the magnetic observatories Boulder, Tucson, and Newport (Figure 1). Although these stations are many hundreds of kilometers from the California array, our experience has shown [Davis et al., 1979] that useful coherence exists between daily averages of component and total fields over these distances. This was borne out by the present study. Furthermore, this study showed that better results are obtained using data from observatories of geomagnetic latitude similar to that of the total field array. After using the Newport records, we found that predictors that worked well during solar quiet times failed during storm activity. Conversely, filters based on storm activity were less successful during quiet times. Filters designed

to compromise for both types of activity were significantly less effective than those obtained when only one type was considered. To some extent this was also true for Tucson, whereas the best results were obtained using the Boulder data. Storms which have their currents in the auroral zones apparently have similar effects at Boulder, Tucson, and the California array. The same is true for variation during quiet times, which arises from lower latitudes. In contrast, because of Newport's higher latitude, storm amplitudes there are larger relative to S_q variation. Consequently, we restricted our analysis to the Boulder records obtained at a mean magnetic latitude nearer to that of the California array.

The Fischer F test was used to test the relative significance of the Weiner coefficients. In all cases statistically significant coefficients were found only at zero lag, which minimized

$$\phi = \sum_{i=1}^n [\delta D_i - (A\delta X_i + B\delta Y_i + C\delta Z_i)]^2 \quad (1)$$

When this occurs,

$$\delta D_i \approx A\delta X_i + B\delta Y_i + C\delta Z_i \quad (2)$$

where δD_i are detrended daily difference field readings over a time interval of n days, δX_i , δY_i , δZ_i are detrended component fields from Boulder, and A , B , C , are zero-lag Weiner filter coefficients which fit the component fields to the differences in a least squares sense. Difficulty in defining these coefficients

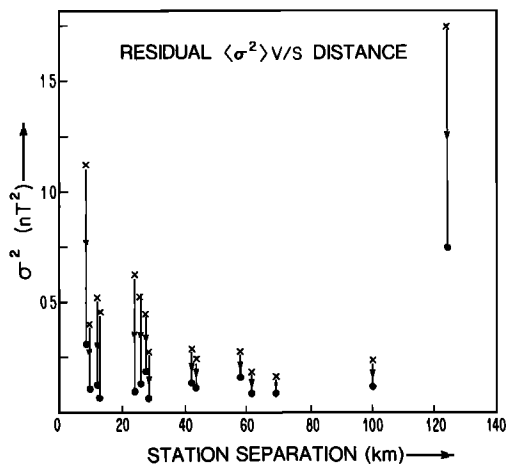


Fig. 2. Variance of magnetic difference fields plotted as a function of station separation. Crosses are the variances before cleaning. Dots are the variances after cleaning. The cleaned variances show no dependence on station separation.

arises from the varying quality of the difference field data through the record. Quality is determined both by gaps in the data and the fraction of the total data for a given day which makes up the daily average. Also, variable trends in the differenced data (see Figure 3) not seen in the observatory fields can bias the coefficients determined from long stretches of data. These effects may be reduced by high-pass filtering, using a Butterworth filter prior to the least squares fitting [Davis *et al.*, 1979]. However, better results were obtained by first segmenting the data into 50-day intervals and then, having identified those containing predictable energy, doing a lumped prediction from the corresponding observatory segments. In this approach, we first determined the prediction quality factor (proportion of the variance in the differences predicted by the linear combination of the observatory components) for each 50-day interval. When a factor greater than 0.5 was obtained, the start and end times were recorded. Since the intervals were detrended and the filters were zero phase, it was possible to string all successful 50-day segments together for the lumped prediction for each station pair. The resulting coefficients were optimal for predicting fluctuations over the whole length of the record. The method has the advantage that the coefficients are determined on portions of the record with good correlation as determined from the first step. Detrended 50-day segments are effectively high-pass filtered, so coefficients are not biased by variable trends. The inclusion of many storm-related segments allows an optimum number of polarity directions of geomagnetic activity to be used in the matching and unique coefficients to be found for a given pair of sites. Of the 36 difference fields analyzed in this way, 15 were found with 50-day segments containing power which was at least 50% and in some cases up to 90% predictable.

The final step in the cleaning process is to subtract the linear combination of the observatory components from the raw difference fields. However, for this step no detrending or high-pass filtering is applied. Since significant coefficients were obtained only at zero lag (implying frequency independence), the coefficients determined from the high-frequency analysis described above are equally applicable at low frequencies. If the long-term secular variation at the observatory is nearly equal to that at the proton sites, the subtraction removes any apparent secular variation induced in the earth's crust.

However, because of its distance from California, both the

secular variation and storm activity at Boulder, though similar in form, are consistently different in amplitude from what would be measured by a Californian observatory. We therefore converted the Boulder magnetic variations to approximate Californian ones by comparing them to 1974 data from Castle Rock observatory (Castle Rock observatory was closed after 1974). High-frequency X and Y field variations were found to be within 3% and 6% of each other, respectively, with Z field variations 20% smaller in California. Long-term trends at Boulder ($\dot{X} = 2$ nT/yr, $\dot{Y} = -45$ nT/yr, $\dot{Z} = -66$ nT/yr) were higher than those from California ($\dot{X} = 2$ nT/yr, $\dot{Y} = -30$ nT/yr, $\dot{Z} = -45$ nT/yr). The conversion therefore consists of reducing the high-frequency Z fluctuations by 20% and correcting the secular variation trends to the Californian values. The appropriate coefficients for component fluctuations measured in California would be approximately equal to those determined from the Boulder high-frequency data with the Z coefficient, C , increased by 20%. This has the net result of both retaining the high-frequency cleaning effects and correcting some of the low-frequency trends. Also, the converted coefficients may be used to infer magnetic properties of the Californian sites, as is shown later.

Figure 2 shows the variances of the 15 difference fields before and after predictive cleaning, plotted as a function of station separation. The cleaned variances show virtually no dependence on station separation, compared to the increased variance with separation for hourly averages reported by Mori and Yoshino [1970]. In our case there is no corresponding increase for daily averages. However, our data differ from theirs in that the predictable energy has been removed and the range of distances is smaller. At large distances the source geometry of currents in the ionosphere and magnetosphere becomes important. The residual variance of 0.1 nT² (which corresponds to a standard deviation of 0.3 nT) is significantly larger than expected from instrumental noise alone (0.25 nT averaged over 144 data = 0.02 nT). The difference is probably due to a combination of inadequacies in the cleaning technique, intrinsic instrumental noise larger than 0.25-nT resolution value, and any localized tectonomagnetic field changes.

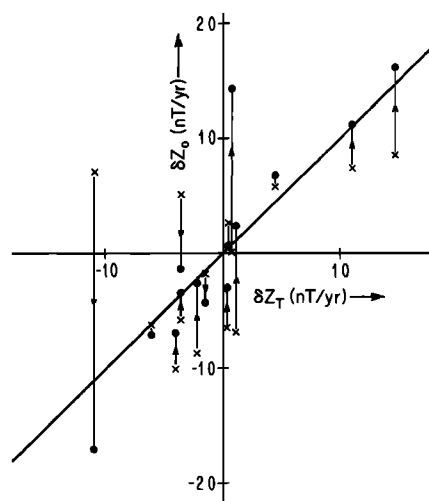


Fig. 3. Annual observed secular variation δZ_0 for daily average difference field records before (crosses) and after (dots) cleaning plotted against the expected secular variation determined from an average of the whole array (δZ_T). The convergence of the cleaned values with the expected variation (solid line) implies that the transfer functions determined for the observatory component fields from the high-frequency fluctuations are applicable at low frequencies.

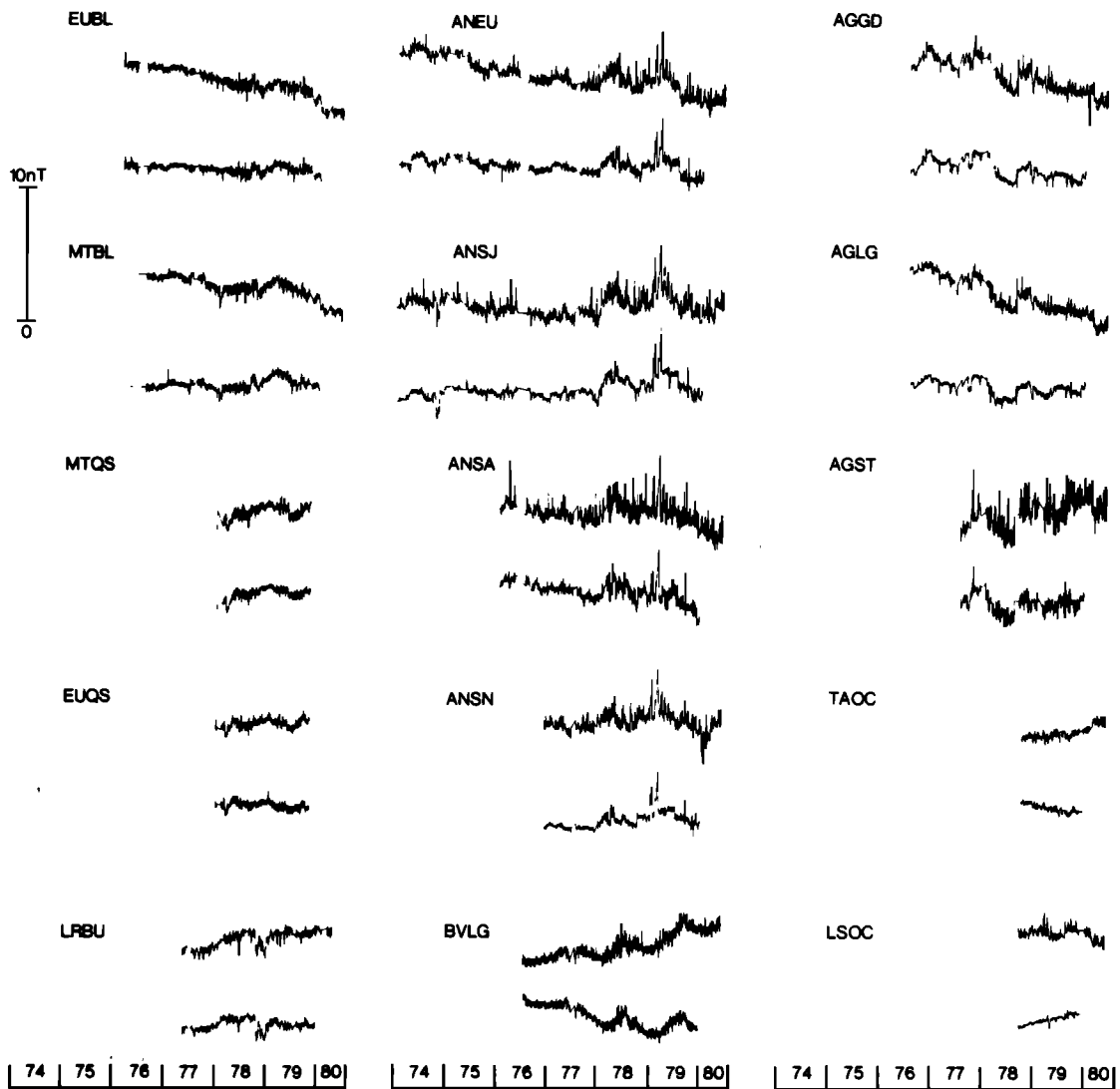


Fig. 4. Daily averages of magnetic difference field records before processing (upper trace) and after processing (lower trace). The processing not only removes high-frequency fluctuations but also corrects trends for effects of variable crustal magnetization in the crust and nonuniform secular variation.

ELIMINATION OF DIFFERENCE FIELD CHANGES
DUE TO CURRENTS IN THE CORE

Silverman and Johnston [1980] have shown that nonuniform secular variation occurs in the total field records from the array, with fields at low latitudes decreasing faster than those at higher latitudes (on average by 1.5 nT/yr/100 km north) with a smaller dependence on longitude. The differences in total fields will undergo corresponding secular trends which, from a least squares analysis of all the total field array data, are given by

$$\delta Z_T = 0.043(\phi_2 - \phi_1) - 2.22(\theta_2 - \theta_1) \quad (3)$$

where δZ_T is the annual secular variation in the difference field between two sites of latitudes θ_1, θ_2 and longitudes ϕ_1, ϕ_2 . Differences are taken station 1 minus station 2. The observed annual secular variations, Z_0 , in the long-term difference field before and after predictive cleaning, are plotted in Figure 3 against the expected values given by (3). In almost every case the trends lie closer to the average for the array after cleaning than before. This improvement gives us some confidence that the coefficients determined from the high-

frequency analysis, based on external field fluctuations, are correctly eliminating low-frequency effects due to induction in a crust of varying susceptibility by fields from core sources.

RESULTS OF CLEANING PROCEDURE

Figure 4 shows the raw traces for each of the 15 difference fields used in Figures 2 and 3, and below each raw trace is its processed version. The processing first removes the high-frequency fluctuations and the crustal component of the apparent secular variation using Wiener filters. Then it removes nonuniform secular variation with (3). Apart from the noise reduction, which is particularly evident on the records differenced with AN, AG, and OC, the trends in the processed records are considerably reduced, on average being close to zero. At this stage, we cannot say that the remaining trends are real, since they depend critically on the accurate determination of the coefficients $A, B,$ and C which, for short records such as TAOC and LSOC, are not well determined. For other records with a low level of predictable energy (e.g., BVLG), $A, B,$ and C need further refining as longer records accrue. Clearly, such refinement will be a major step for long-term monitor-

ing purposes. Here we have detrended subsequent plots because of this uncertainty.

THE ORIGIN OF THE FREQUENCY-INDEPENDENT INDUCTION EFFECTS

Since only zero-lag filter coefficients were required to effect significant cleaning, the transfer functions between the component fields and the difference fields are frequency independent. Frequency-dependent electromagnetic induction has a skin depth given by

$$Z_s = (2/\omega\mu\sigma)^{1/2}$$

where σ is the conductivity, ω is the angular frequency, and μ is the permeability of the crust. If ω corresponds to a frequency of one cycle per day and using representative values of crustal and upper mantle rocks for μ and σ ($\mu = 4\pi \times 10^{-7}$ W/m², $\sigma = 10^{-2}$ S/m), the skin depth Z_s is 1500 km. Induced currents at this and longer periods will be distributed over large scales in the crust and upper mantle and are unlikely to cause appreciable magnetic field gradients over distances of tens of kilometers other than in cases of exceptional current channeling. Frequency independent effects arise from two sources: (1) variable crustal susceptibility giving rise to contrasting magnetic induction at sites, and (2) combined variable remanence and susceptibility which leads to nonparallel total fields so that vector addition of a uniform disturbance field is unequal at each site. We refer to these as susceptibility and orientation effects respectively.

The assumption that the disturbance field originating in the ionosphere is uniform at pairs of sites needs to be justified. Since our study shows that only 15 of 36 difference fields have energy correlated with external magnetic activity, the success of the differencing technique for the remaining 21 is most readily explained by spatially uniform disturbances that cancel on differencing. The cancelling only partly succeeds where crustal magnetic heterogeneity is present.

The orientation effect can be quantified as follows. Let I_1 , D_1 and I_2 , D_2 be the inclination and declination at each of two sites 1 and 2. To a first-order approximation the change in the difference field, $D = |T_1| - |T_2|$, corresponding to a uniform disturbance field (δX , δY , δZ), is

$$\begin{aligned} \delta D = & (\cos D_1 \cos I_1 - \cos D_2 \cos I_2)\delta X \\ & + (\sin D_1 \cos I_1 - \sin D_2 \cos I_2)\delta Y \\ & + (\sin I_1 - \sin I_2)\delta Z \end{aligned} \quad (4)$$

This may be rewritten as

$$\delta D = \zeta(\delta X\beta_1 + \delta Y\beta_2 + \delta Z\beta_3) \quad (5)$$

where ζ is the angle between the total field vectors and (β_1 , β_2 , β_3) are the direction cosines of the difference vector $\vec{T}_1 - \vec{T}_2$, i.e., between the total fields \vec{T}_1 and \vec{T}_2 .

To quantify effects of magnetic induction, we choose a spherical polar coordinate system with \vec{r} in the direction of \vec{T}_2 (Figure 5). Since in all cases $|\vec{T}_1| \approx |\vec{T}_2|$ and ζ is small, $\vec{T}_1 - \vec{T}_2$ is nearly perpendicular to \vec{T}_2 and is thus almost coincident with the θ axis. Then $\vec{\phi}$ is taken at right angles to both \vec{r} and $\vec{\theta}$ (in the direction $\vec{r} \times \vec{\theta}$). M_{ij} is defined as the field induced in the i direction at site 1 by a uniform disturbance field in the j direction observed at site 2, where a contrast in susceptibility between the two sites causes induction. A disturbance (ΔH_r , ΔH_θ , ΔH_ϕ) will induce (δH_r , δH_θ , δH_ϕ) given by

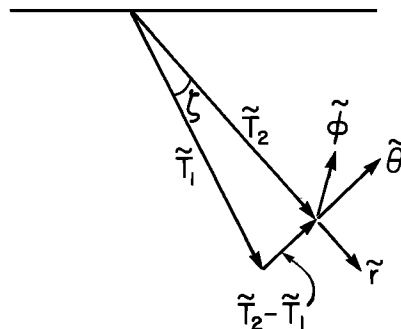


Fig. 5. Geometry used for calculation of magnetic induction effects in total field differences $|\vec{T}_1| - |\vec{T}_2|$ between two proton magnetometer sites.

$$\begin{bmatrix} \delta H_r \\ \delta H_\theta \\ \delta H_\phi \end{bmatrix} = \begin{bmatrix} M_{rr} & M_{r\theta} & M_{r\phi} \\ M_{\theta r} & M_{\theta\theta} & M_{\theta\phi} \\ M_{\phi r} & M_{\phi\theta} & M_{\phi\phi} \end{bmatrix} \begin{bmatrix} \Delta H_r \\ \Delta H_\theta \\ \Delta H_\phi \end{bmatrix} \quad (6)$$

For future reference we call M_{ij} the field susceptibility matrix, which is symmetric, i.e., $M_{ij} = M_{ji}$. The resulting perturbation in the difference field δD from contrasting susceptibility is δH_r , since δH_θ and δH_ϕ contribute negligibly, i.e.,

$$\delta D = M_{rr} \Delta H_r + M_{r\theta} \Delta H_\theta + M_{r\phi} \Delta H_\phi \quad (7)$$

To this perturbation we must add the contribution from the orientation effect in (5), i.e.,

$$\delta D = M_{rr} \Delta H_r + (M_{r\theta} + \zeta)\Delta H_\theta + M_{r\phi} \Delta H_\phi \quad (8)$$

If we expand this expression in terms of δX , δY , and δZ , we can use (1) to find M_{rr} , $M_{r\theta}$, and $M_{r\phi}$ in terms of A , B , and C . Let the direction cosines of \vec{T}_2 be (α_1 , α_2 , α_3) given by

$$\begin{aligned} \alpha_1 = \cos I_2 \cos D_2 & \quad \alpha_2 = \cos I_2 \sin D_2 \\ \alpha_3 = \sin I_2 & \end{aligned} \quad (9)$$

The direction cosines of the ϕ direction are then

$$\begin{aligned} v_1 = \alpha_2\beta_3 - \beta_2\alpha_3 & \quad v_2 = \alpha_3\beta_1 - \alpha_1\beta_3 \\ v_3 = \alpha_1\beta_2 - \beta_1\alpha_2 & \end{aligned} \quad (10)$$

and we then get for δD

$$\begin{aligned} \delta D = & \alpha_1 M_{rr} \delta X + \alpha_2 M_{rr} \delta Y + \alpha_3 M_{rr} \delta Z \\ & + \beta_1 (M_{\theta r} + \zeta) \delta X + \beta_2 (M_{\theta r} + \zeta) \delta Y + \beta_3 (M_{\theta r} + \zeta) \delta Z \\ & + v_1 M_{\phi r} \delta X + v_2 M_{\phi r} \delta Y + v_3 M_{\phi r} \delta Z \end{aligned} \quad (11)$$

Therefore

$$\begin{aligned} A = & \alpha_1 M_{rr} + \beta_1 (M_{\theta r} + \zeta) + v_1 M_{\phi r} \\ B = & \alpha_2 M_{rr} + \beta_2 (M_{\theta r} + \zeta) + v_2 M_{\phi r} \\ C = & \alpha_3 M_{rr} + \beta_3 (M_{\theta r} + \zeta) + v_3 M_{\phi r} \end{aligned} \quad (12)$$

These equations are readily solved to yield

$$\begin{aligned} M_{rr} = & A\alpha_1 + B\alpha_2 + C\alpha_3 \\ M_{\theta r} = & A\beta_1 + B\beta_2 + C\beta_3 - \zeta \\ M_{\phi r} = & Av_1 + Bv_2 + Cv_2 \end{aligned} \quad (13)$$

which enables us to calculate the elements in the top row of the field susceptibility matrix using the A , B , C determined from the filtering analysis and the direction cosines determined from measurements of the static fields.

TABLE 1. Values of the Filter Coefficients Which, When Multiplied by the Component Field Variations Measured at Boulder Magnetic Observatory, Predict the Total Field Differences at the Sites of the California Array.

		A	B	C
AN	SA	-0.0284	-0.0115	0.0013
AN	SN	-0.0221	-0.0091	0.0069
AG	LG	-0.0166	0.0011	0.0049
AG	GD	-0.0204	0.0025	0.0074
BV	LG	-0.0165	0.0170	0.0148
EU	BL	0.0140	-0.0017	-0.0008
AG	ST	-0.0352	0.0009	0.0258
LR	BU	0.0165	-0.0128	-0.0046
LS	OC	-0.0152	0.0014	0.0146
TA	OC	0.0034	-0.0098	-0.0209
MT	BL	0.0142	-0.0023	-0.0013
AN	EU	-0.0228	-0.0074	0.0053
AN	SJ	-0.0284	-0.0060	0.0114
MT	QS	-0.0109	0.0133	0.0063
EU	QS	-0.0101	0.0022	0.0070

STATIC DIFFERENCE FIELDS

We can calculate the components of the difference fields between the two sites due to induction ($H_{I_r}, H_{I_\theta}, H_{I_\phi}$), and subtract them from the measured differences (H_r, H_θ, H_ϕ) to give the components of the difference fields from remanence ($H_{R_r}, H_{R_\theta}, H_{R_\phi}$). For our chosen geometry, let H_0 be the value of $|\vec{T}_2|$. Then, in (6), $\Delta H_r = H_0, \Delta H_\theta = 0 = \Delta H_\phi$ so that

$$H_{I_r} = M_{rr}H_0$$

and, owing to symmetry of the field susceptibility matrix,

$$H_{I_\theta} = M_{\theta r}H_0 = M_{r\theta}H_0 \quad H_{I_\phi} = M_{\phi r}H_0 = M_{r\phi}H_0$$

giving

$$\begin{aligned} H_{R_r} &= H_r - M_{rr}H_0 \\ H_{R_\theta} &= H_\theta - M_{r\theta}H_0 = (\zeta - M_{r\theta})H_0 \\ H_{R_\phi} &= H_\phi - M_{r\phi}H_0 = -M_{r\phi}H_0 \end{aligned} \tag{14}$$

TABLE 2. Declination and Inclinations at Sites of the California Total Field Magnetometer Array

	Declination D , deg	Inclination I , deg
BL	16.1979	61.6366
MT	16.2062	61.3805
EU	15.8326	61.3931
CO	15.9795	61.3389
SA	16.1500	61.1430
NA	15.4932	61.2493
AN	15.4153	61.9042
SN	15.7712	61.1569
SJ	15.8246	60.9840
HA	15.7267	60.9514
LE	15.9095	60.7972
BV	15.8784	60.8465
LG	15.3033	59.9320
GD	15.0419	60.1972
AG	15.7709	60.9458
GR	15.3044	60.2000
ST	14.9835	59.6696
AB	15.3662	59.7042
CH	14.4236	59.7639
PA	14.4028	59.7361
BU	14.5679	60.1708
LR	14.3913	59.5708
OC	14.4373	59.3361
LS	14.4817	59.8930
TA	13.7306	58.8681
BC	13.7279	59.0739

since $\zeta = H_\theta/H_0$ and, for the chosen geometry, $H_\phi = 0$. We can now separate the components of the difference fields between two sites into contributions from both remanence and susceptibility. Since the magnetic fluctuations from storm activity have provided a known forcing function, we can estimate the susceptibility contrast. Numerical values are given in the next section.

EVALUATION OF THE COMPONENTS OF REMANENT AND INDUCED DIFFERENCE FIELDS BETWEEN SITES

Values of $A, B,$ and C for the differenced pairs are shown in Table 1. Least squares estimates of the standard deviations range from a few percent to 20%. We proceed by assuming that effects of electromagnetically induced current channeling are small at the long periods (days-years), and across the short distances (tens of kilometers) over which magnetic differences are taken.

Inclinations and declinations were measured at all sites (except for QS) of the California array in 1981 using a magnetic theodolite. These measurements are listed in Table 2. Inclinations were measured relative to the vertical as determined from levels. Declinations were measured relative to true north by taking sun shots. Repeated measurements at several sites indicates an accuracy of 0.03° for inclinations and 0.1° for declination.

Values of $M_{rr}, M_{\theta r},$ and $M_{\phi r}$ from (13) are listed in Table 3. Also listed is $M_\perp = M_{\theta r} + \zeta$, i.e., the fraction of a perturbation comprised of both the susceptibility and orientation effect in the $\hat{\theta}$ direction which appears in the total field differences. The remaining seven columns in the table are the induced components of the difference fields ($H_{I_r}, H_{I_\theta}, H_{I_\phi}$) from (14), the remanent components of the difference fields ($H_{R_r}, H_{R_\theta}, H_{R_\phi}$), and finally the differences in total fields.

DISCUSSION

The results of Table 3 show that total field differences are most dependent on perturbations in the θ direction since M_\perp is on average a factor of 6 greater than M_{rr} . This occurs because the orientation effect is several times stronger than the effect of magnetic induction. Also, since in every case but one $M_{\theta r}$ is positive, the susceptibility and orientation effects reinforce each other. For the static fields, the earth's field in the \hat{r} direction induces a field in the $\hat{\theta}$ direction giving rise to the misalignment. Due to the symmetry of M_{ij} , a disturbance in the $\hat{\theta}$ direction then induces a change in the \hat{r} direction which, along with the orientation effect, is detected on differencing.

That changes directed along the difference vector of total fields are likely to be primarily responsible for fluctuations in the difference field record can explain results not previously understood. In 1966, T. Rikitake proposed a method of cleaning total field differences which consisted of forming a weighted difference with the weight determined from linear regression. However, the success of this technique has been limited [Rikitake, 1966; Mori and Yoshino, 1970; Davis and Searls, 1981; Johnston et al., 1981]. Other work has shown [Davis et al. 1981] that the most important components for reducing noise in southern California differences were the vector components orthogonal to the field-aligned direction. This dependence is expected from the foregoing analysis, since these components contain information on the fluctuations in the direction of the difference vector, whereas Rikitake's method uses fluctuations which are orthogonal to it. Prediction of one

TABLE 3. Magnetic Parameters Pertaining to Remanence and Induced Fields at Stations of the California Array

		M_{rr}	$M_{\theta r}$	$M_{\phi r}$	M_{\perp}	H_{Ir}	$H_{I\theta}$	$H_{I\phi}$	H_{Rr}	$H_{R\theta}$	$H_{R\phi}$	Differences in Total Fields
AN	SA	-0.013	0.0118	-0.0085	0.0264	-651.0	-588.0	-427.0	883.0	143.0	427.0	232.0
AN	SN	-0.0039	0.0114	-0.0027	0.0248	-195.0	572.0	-137.0	277.0	96.0	137.0	82.0
AG	LG	-0.0025	-0.0008	-0.0017	0.0174	-124.0	-39.0	-84.0	286.0	946.0	84.0	162.0
AG	GD	-0.0015	0.0078	0.0020	0.0222	-73.0	388.0	99.0	435.0	336.0	-99.0	362.0
BV	LG	0.0100	0.0072	-0.0144	0.0240	498.0	362.0	-719.0	-361.0	473.0	719.0	137.0
EU	BL	0.0054	0.0076	0.0024	0.0129	269.0	381.0	121.0	-142.0	-120.0	-121.0	127.0
AG	ST	0.0107	0.0224	0.0032	0.0456	536.0	1118.0	161.0	-131.0	47.0	-161.0	405.0
LR	BU	0.0017	0.0055	-0.0143	0.0161	85.0	275.0	-716.0	-673.0	254.0	716.0	-588.0
LS	OC	0.0079	0.0117	-0.0043	0.0214	397.0	586.0	-215.0	-1064.0	-100.0	215.0	-667.0
TA	OC	-0.0210	0.0068	0.0003	0.0171	-1051.0	340.0	16.0	2586.0	177.0	-16.0	1535.0
MT	BL	0.0049	0.0076	-0.0064	0.0121	243.0	380.0	-318.0	14.0	-156.0	318.0	257.0
AN	EU	-0.0057	0.0133	-0.0078	0.0228	-285.0	663.0	-391.0	405.0	-185.0	391.0	120.0
AN	SJ	-0.0016	0.0145	-0.0085	0.0309	-80.0	724.0	-424.0	160.0	97.0	424.0	80.0

Measurements in nT. See text for definitions.

difference pair from another, as suggested by *Ware* [1979], will also not work in general because the difference vectors in each case are unlikely to be colinear.

This result has the practical implication that many historical data should be reanalyzed using observatory components to reduce noise. Reanalysis may reveal anomalies hidden from view due to the noise level. In general, the induced and remanent difference fields of Table 3 are of the same order of magnitude. This means that models of these California magnetic anomalies will be incomplete if remanence is not taken into account. Figure 6 shows all 36 difference fields from the U.S. Geological Survey over the interval 1974–1980, with the 15 cleaned difference fields replacing the raw records where appropriate.

All records have been detrended. Times of the Busch fault and Coyote earthquakes are depicted by the vertical dashed lines. Two anomalous periods stand out in the data. On all records up to the beginning of 1978 the 1974 Busch fault variation seen on differences with SJ is the largest event. However, after 1978, many records show equally large variations, the most significant of which occur in differences taken with AN. These variations reach a peak in early 1979 and exhibit a sharp offset several weeks before the Coyote earthquake. In addition, differences with HA early in 1979 exhibit a marked trend reversal and step just weeks before the Coyote earthquake followed by a resumption of the original trend. Both of these stations are within 50 km of the epicenter.

Other variations which stand out above the background noise level include the transient offset in differences with AG in mid-1978 and the transient offset in differences with BU late in 1978. The cyclical, annual variation in records such as MTCO, SJBV, STAB, CHAB, which appears to correlate with either annual temperature or magnetic field changes, has not been satisfactorily explained by temperature sensitivity of the instruments. Experiments involving temperature cycling of the instruments, over a 20°C range, produced no measurable perturbation in the record. However, since the magnetic records do correlate with an annual variation, a precursive interpretation of the fluctuations, e.g., prior to the earthquake of August 6, 1979, seems unreasonable. There is also no evidence of a coseismic offset in the magnetic records at the time of the earthquake. *Johnston et al.* [1981] have shown with model calculations that the expected coseismic anomaly is below the measurement resolution. Their model consists of a strike-slip fault 23 km long by 10 km deep in which an average stress change of 10 bars occurs.

Stations on which we see anomalous variation, HA and AN, lie 50 km and 30 km, respectively, from the Coyote earthquake and in the transition region between the creeping section of the San Andreas fault to the south and the locked section to the north. If the anomalies relate to stress changes in this region, the changes are larger than those released by the earthquake. Lack of coherence between changes seen at HA and AN and the lack of any sizable anomaly at SJ or LE indicate a very uneven stress accumulation.

Arguments that the remaining fluctuations of Figure 6 are due to crustal stress changes include: (1) the proximity in both space and time of the Busch fault anomalies to the Busch fault earthquake and (2) the increase in anomalous activity beginning in 1978–1979, which corresponds to the increase in California seismic activity following the 1975.7–1978.7 seismic lull [*Bufe and Topozada*, 1981]. This increase includes offsets in HA and AN just prior to the Coyote earthquake.

CONCLUSIONS

Magnetic observatory data from Boulder, Colorado have been used to reduce noise in the difference fields between proton magnetometers of the U.S. Geological Survey array in California. Observatory data from Newport were less successful because Newport is at a higher latitude than the array and so experiences different magnetic activity. Of 36 difference fields tested, 15 contained sections of record for which the power predicted from the observatory components was greater than 50% of the total. They correspond to 8 of the 23 stations from which the differences were derived. The differences show markedly different trends after cleaning than before and agree better with the mean secular variation of the array. In three cases cleaning reverses the trends which, if unaccounted for, could lead to wrong conclusions about the sense and size of stress buildup at those sites.

A combination of orientation and susceptibility effects causes the predictable variations in the difference fields. A fraction of the disturbance fields in the direction of the difference vector appears in the differences because of unequal vector addition of the disturbance field to the total fields. This is the orientation effect. Induced fields differ also at sites of contrasting susceptibility. For pairs of sites where the total fields have different orientations explained by contrasting susceptibility, the field susceptibility tensor has a large off-diagonal component. Disturbances in the direction of the difference vector induce large changes in the total field direction which appear in the difference field record. Eliminating these

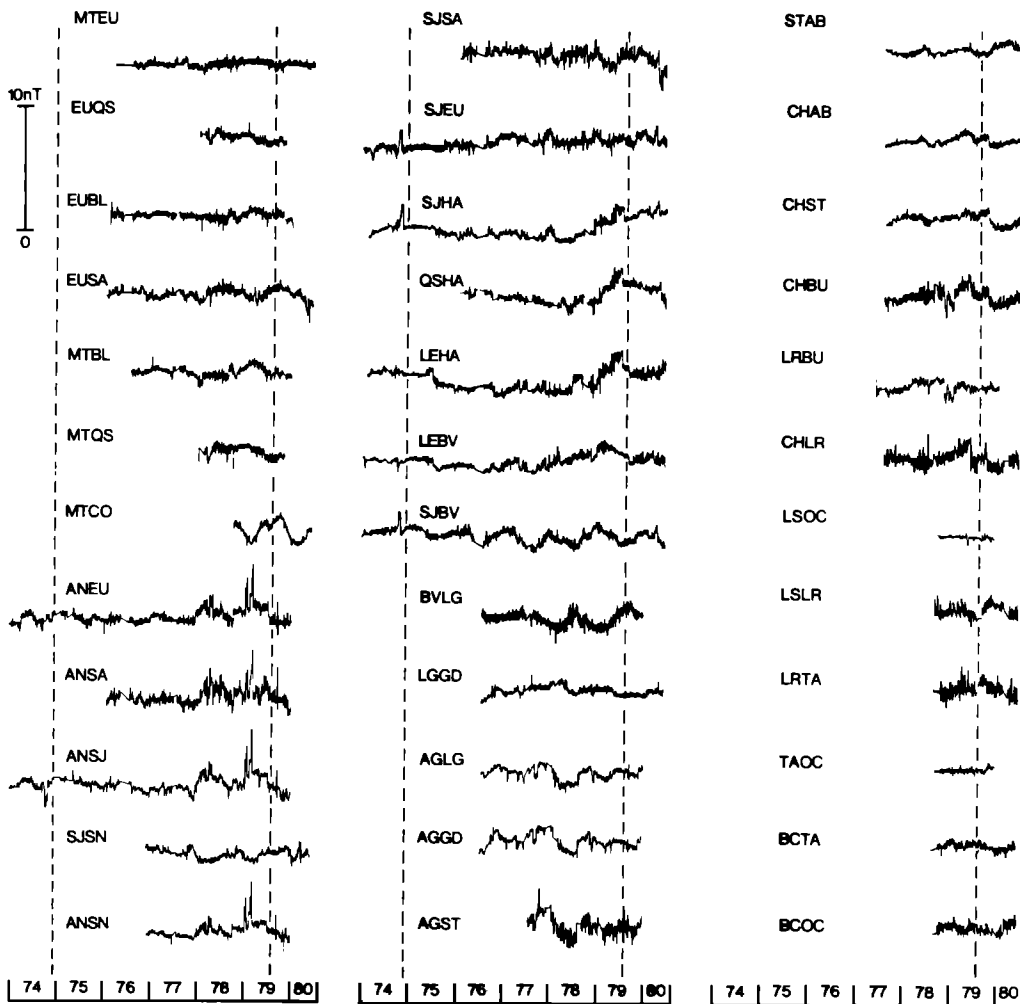


Fig. 6. Daily averages of detrended difference fields from 23 stations of the U.S. Geological Survey array for the period 1974–1980 with the processed data (Figure 4) replacing raw data where applicable. Times of the Busch fault (1974) and Coyote earthquakes (1979) are marked by dashed lines.

changes requires information in the direction of the difference vector, i.e., perpendicular to the total field direction. This requirement reveals why all cleaning methods solely dependent on total field information alone have had only slight success.

Examination of residual fluctuations after cleaning shows that the magnetic variation before the Busch fault earthquake can still be regarded as an anomalous excursion. Similar, larger variations which may be related to the Coyote earthquake are seen in 1978–1979. Variations of several nT are seen at stations AN and HA, 30 and 50, km, respectively, south of the earthquake epicenter, with offsets appearing several weeks before the event. However, the records of CO within a few kilometers of the event are not similarly affected.

The absence of coseismic magnetic events greater than 0.25 nT and the presence of aseismic excursions of several nT in the records, if piezomagnetically induced, indicate that stress accumulation and relaxation are an order of magnitude greater than coseismic stress release and concentrate in an irregular manner along the San Andreas fault.

Acknowledgments. R. Mueller provided invaluable technical support. John Evans and an anonymous associate editor provided useful review comments. P. M. Davis acknowledges support from U.S. Geological Survey grant 14-08-0001-19246. The World Data Center A for Solar-Terrestrial Physics provided magnetic observatory records, and

John Walker of the Department of Energy, Mines, and Resources, Ottawa, Canada arranged the loan of the magnetic theodolite.

REFERENCES

- Bufe, C. G., and T. R. Topozada, California earthquakes: End to seismic quiescence, *Calif. Geol.*, **34**, 111–114, 1981.
- Davis, P. M., and C. S. Searls, Magnetic field measurements in the aftershock region of the Coyote Lake earthquake, *J. Geophys. Res.*, **86**, 927–930, 1981.
- Davis, P. M., F. D. Stacey, C. J. Zablocki, and J. Olson, Improved signal discrimination in tectonomagnetism: Discovery of a volcanomagnetic effect on Kilauea, Hawaii, *Phys. Earth Planet. Inter.*, **19**, 331–336, 1979.
- Davis, P. M., D. D. Jackson, and M. J. S. Johnston, Further evidence of localized geomagnetic field changes before the 1974 Thanksgiving Day earthquake, Hollister, California, *Geophys. Res. Lett.*, **7**, 513–516, 1980.
- Davis, P. M., D. D. Jackson, C. S. Searls, and R. L. McPherron, Detection of tectonomagnetic events using multichannel predictive filtering, *J. Geophys. Res.*, **86**, 1731–1737, 1981.
- Johnston, M. J. S., Local magnetic variations and stress changes near a slip discontinuity on the San Andreas fault, *J. Geomagn. Geoelectr.*, **30**, 511–522, 1978.
- Johnston, M. J. S., R. J. Mueller, and V. Keller, Preseismic and coseismic magnetic field measurements near the Coyote Lake, California, earthquake of August 6, 1979, *J. Geophys. Res.*, **86**, 921–926, 1981.
- Mori, T., and T. Yoshino, Local difference of the geomagnetic total intensity in Japan, *Bull. Earthquake Res. Inst. Univ. Tokyo*, **48**, 893–922, 1970.

- Rikitake, T., Elimination of non-local changes from total intensity values of the geomagnetic field, *Bull. Earthquake Res. Inst. Univ. Tokyo*, *44*, 1041–1070, 1966.
- Silverman, S., and M. J. S. Johnston, Have large-scale magnetic changes of crustal origin occurred within the San Andreas fault system, 1974–1980?, *Eos Trans. AGU*, *61*, 1118, 1980.
- Smith, B. E., and M. J. S. Johnston, A tectonomagnetic effect observed before a magnitude 5.2 earthquake near Hollister, California, *J. Geophys. Res.*, *81*, 3556–3560, 1976.
- Ware, R. H., High-accuracy magnetic field difference measurements and improved noise reduction techniques for use in tectonomagnetic studies, *J. Geophys. Res.*, *84*, 6291–6295, 1979.
-
- P. M. Davis, Department of Earth and Space Sciences, University of California, Los Angeles, CA 90024.
- M. J. S. Johnston, U.S. Geological Survey, 345 Middlefield Road, Menlo Park, CA 94025.

(Received August 3, 1982;
revised June 16, 1983;
accepted June 17, 1983.)